



HAL
open science

Cartography of the mechanical properties of the human amniotic membrane

Agathe Gremare, Sarah Jean-Gilles, Pauline Musqui, Laure Magnan, Yoann Torres, Mathilde Fenelon, Stéphanie Brun, Jean-Christophe Fricain, Nicolas L'heureux

► **To cite this version:**

Agathe Gremare, Sarah Jean-Gilles, Pauline Musqui, Laure Magnan, Yoann Torres, et al.. Cartography of the mechanical properties of the human amniotic membrane. *Journal of the mechanical behavior of biomedical materials*, 2019, 99, pp.18-26. 10.1016/j.jmbbm.2019.07.007 . inserm-02870489

HAL Id: inserm-02870489

<https://inserm.hal.science/inserm-02870489>

Submitted on 25 Oct 2021

HAL is a multi-disciplinary open access archive for the deposit and dissemination of scientific research documents, whether they are published or not. The documents may come from teaching and research institutions in France or abroad, or from public or private research centers.

L'archive ouverte pluridisciplinaire **HAL**, est destinée au dépôt et à la diffusion de documents scientifiques de niveau recherche, publiés ou non, émanant des établissements d'enseignement et de recherche français ou étrangers, des laboratoires publics ou privés.



Distributed under a Creative Commons Attribution - NonCommercial 4.0 International License

1. Title page

Title: Cartography of the mechanical properties of the Human Amniotic Membrane

Agathe Grémare^{1,2}, Sarah Jean-Gilles³, Pauline Musqui², Laure Magnan¹, Yoann Torres¹, Mathilde Fénelon^{1,2}, Stéphanie Brun⁴, Jean-Christophe Fricain^{1,2}, Nicolas L'Heureux¹

¹ Univ. Bordeaux, INSERM, Tissue Bioengineering, U1026, F-33076 Bordeaux, France

² CHU Bordeaux, Odontology and Oral Health Department, F-33076 Bordeaux, France

³ Univ. Cergy-Pontoise, F-95000 Cergy-Pontoise, France

⁴ CHU Bordeaux, Gynecology-Obstetrics Service, F-33076 Bordeaux, France

Corresponding author:

Nicolas L'Heureux

Laboratory for the Bioengineering of Tissues (BioTis), Inserm U1026

Campus Carreire

146 rue Léo Saignat, Zone Nord, Bat 4A, 2^{ème} étage

33076 Bordeaux Cedex France

Contact telephone number: 33 (0)5 57 57 17 23

FAX number: 33 (0)5 56 90 05 17

e-mail: nicolas.lheureux@inserm.fr

2. Abstract and key terms

Abstract:

Because of its low immunogenicity, biological properties, and high availability, the Human Amniotic Membrane (HAM) is widely used in the clinic and in tissue engineering research. However, while its biological characteristics are well described, its mechanical properties remain understudied especially in terms of inter- and intra-HAM variability. To guide bioengineers in the use of this natural biomaterial, a detailed cartography of the HAM's mechanical properties was performed. Maximal force (F_{max}) and strain at break (S_{max}) were identified as the relevant mechanical criteria for this study after a combined analysis of histological sections, thickness measurements after dehydration, and uniaxial tensile tests. Eight HAMs were studied by mechanical cartography using a standardized cutting protocol and sampling pattern. On average, 103 ± 10 samples were retrieved and tested per HAM. Intra-tissue variability highlighted the fact that there were two mechanically distinct areas (placental and peripheral) in each HAM. For all HAMs, placental HAM was significantly stronger by $82 \pm 45 \%$ and more stretchable by $19 \pm 6 \%$ than their peripheral counterparts. Our results also demonstrated that placental, but not peripheral, HAM presented isotropic mechanical properties. Thus, placental HAM can be a raw material of choice that could be favored especially in the development of tissue engineering products where mechanical properties play a key role.

Key terms:

- Human amnion
- Tissue engineering
- Natural biomaterial
- Mechanical properties
- Mapping

3. Introduction

The human amniotic bag is composed of both amniotic and chorionic membranes. The human amniotic membrane (HAM) corresponds to the innermost membrane⁸. This tissue comprises a connective layer, that is neither vascularized nor innervated, and an epithelial monolayer, which is in direct contact with the amniotic fluid. This epithelium rests on a thin basal membrane rich in collagen type IV, laminin, fibronectin and nidogen. The connective layer is divided into three layers containing collagen types I and III: the inner acellular compact layer, the loose fibroblast layer and the outer spongy layer. The spongy layer of the HAM can be easily delaminated to separate the HAM and the chorion by blunt dissection^{8 30}.

This tissue is routinely discarded *post-partum* and, consequently, is a widely available and cost-effective raw material for medical and tissue engineering applications. Clinically, allogenic HAM has long been used in both ophthalmology, for ocular surface reconstruction²³, and dermatology, for treatment of chronic non-healing wounds¹⁵. These good clinical outcomes are attributed to the HAM's purported low immunogenicity due to the lack of HLA class II antigens^{20 22}. Moreover, this tissue has both anti-inflammatory¹⁴ and anti-microbial effects^{19 18} due to the production of anti-inflammatory proteins (such as IL-1 RA and IL-10) and β -defensins respectively. These qualities have made the HAM particularly attractive as a biological scaffold for tissue engineering³⁰ and has been used for vascular^{1 34}, peripheral nerve²⁷, periodontal^{10 28}, cartilage⁷, and bone regeneration^{11 21} research among others.

Mechanically, this tissue is highly deformable yet strong and withstands the progressive stretching of the growing embryo as well as protects it from external traumas^{4 32}. Oxlund *et al.* demonstrated that the amniotic membrane is largely responsible for the strength of intact fetal membranes³² (Oxlund et al., 1990). Other groups have published detailed studies of the viscoelastic behaviour of this tissue and its intrinsic mechanical properties^{33 4. 17 24}. In this report, we have performed a comparative study using simple mechanical properties to assess the variability within individual HAMs as well as between HAMs of different donors. Indeed, like all biological tissues, a high level of

variability of the mechanical properties of the HAM can be expected. In addition, scientists have shown that HAMs have a distinct weak zone overlying the *cervix*, to facilitate the process of fetal membrane rupture during delivery, with particular biochemical and histological features^{9 26}. Hence, it is critical to assess the variability of the mechanical properties of this natural biomaterial in order to develop effective production strategies for tissue-engineered products relying on its strength. To our knowledge, no study has provided a detailed mechanical cartography of the HAM.

In this study, we developed standardized HAM cutting and HAM sampling protocols that allowed the evaluation of up to 125 samples per membranes to meticulously assess the inter- and intra-tissue variability of its mechanical properties.

4. Materials and methods

4.1 HAM collection

Fetal membranes were collected from eight patients who had a caesarean delivery at term before the initiation of labor. Patients were recruited for this study with informed consent approved by the institutional review board. All patients had mono-fetal pregnancies and were seronegative for Human Immunodeficiency Virus (HIV) 1 and 2 and for Hepatitis B and C viruses. Tissues were kept in ice-cold transport solution containing phosphate buffered solution (PBS 1X, Gibco®) supplemented with 1% penicillin/streptomycin (Gibco®). The next day, negative HIV 1 and 2 serologies were confirmed using a band immunochromatography test (ALERE®, ref: 7D2346) and the samples were collected.

4.2 HAM cutting protocol and sampling pattern

To perform HAM cartographies, a HAM standardized cutting protocol was developed (figure 1). First, the umbilical cord was removed. Tissues were then rinsed with distilled water at least six times. The placenta and its membranes were placed on a large cutting board with the placental long axis oriented horizontally. Before cutting, membranes were spread out and distributed homogeneously on the placenta. They were cut into eight parts with a surgical blade (figure 1B). The first cut was made along the long axis of the placenta, starting at the edge of the placental rim and finishing on the other side of the placental rim. The second cut was made perpendicular to the first in the same way. Then, four additional cuts were performed, at equal intervals to allow the membranes to lay flat. The amnion and the chorion were then separated manually (figure 1C). Finally, the HAM was detached from the placenta (figure 1D). This tissue was then sampled using a dog-bone shaped punch similar to ASTM D-638 type V (maximal width = 7.5 mm, minimal width = 2.5 mm, linear length = 6 mm and overall length = 38.63 mm) following a sampling pattern with two areas (placental and peripheral) and two directions (radial and circumferential) (figure 1E). Wet samples were stored at -20°C.

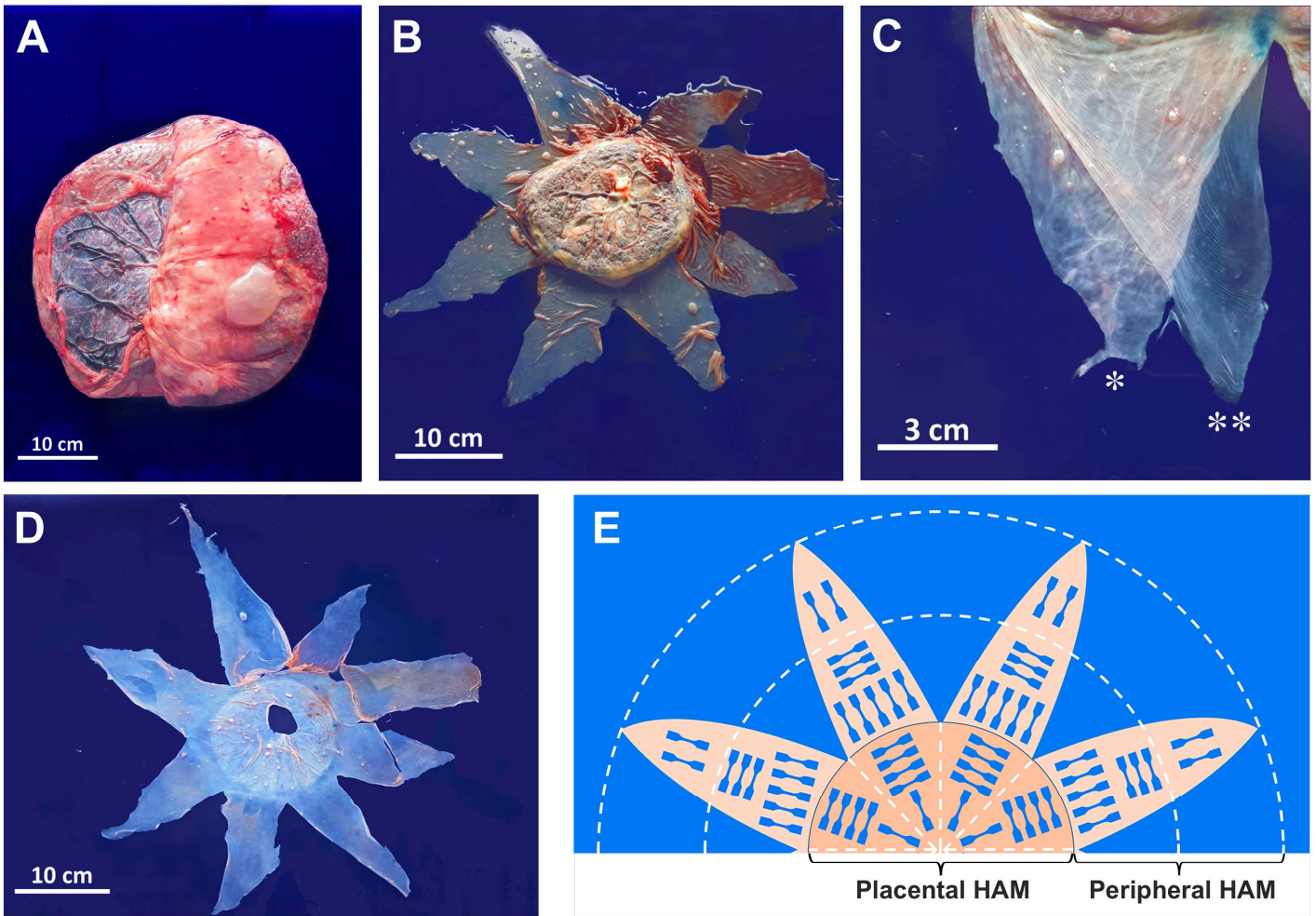


Figure 1: HAM cutting protocol and sampling pattern.

(A) The placenta, umbilical cord and fetal membranes were collected from eight patients who had a caesarean delivery at term. The fetal bag (membranes) is seen on top of the placenta and a surgical incision is clearly visible. (B) The amniochorionic membrane was cut in eight parts (the placenta is at the center under the membrane). (C) The amnion (**) and the chorion (*) were manually separated. (D) The HAM was isolated and spread out. (E) The HAM was sampled in two areas (placental and peripheral HAM) and in two directions (radial and circumferential).

4.3 Histological analysis

Fresh HAM samples were fixed in 4% PFA (Antigenfix®) overnight. After rinses in PBS 1X, HAM samples were rolled, put in a cassette and processed for paraffin embedding. Paraffin sections (5 μm) were deparaffinized in toluene for 3×5 minutes, followed by a descending series of ethanol baths and stained with Masson's trichrome Masson that stains fibrillar collagen specifically in green. Images were acquired using an optical microscope (Nikon®, Eclipse 80i). All samples were treated at the same time and imaged using identical settings to allow staining intensity comparison.

4.4 Thickness measurement

Four square pieces of HAM (0.25 cm^2) were cut with a scalpel. Each piece was put on a metallic tube with a known diameter of 4774 μm . Metallic tube diameter plus HAM thickness were measured using a laser micrometer (Aeroel®, Xactum) to determine HAM thickness.

4.5 Uniaxial tensile test

After thawing (1.5h, at room temperature, in distilled water), uniaxial tensile tests were performed on dog-bone shaped HAM samples using an Autograph AGS-X tensile tester using the Trapezium® software (Shimadzu®) (figure 2A). Care was taken to ensure that samples remained fully hydrated at all times. Distilled water was regularly put on the samples using a brush. HAM samples were pre-loaded at 20 mm/min to 0.1 N (without additional pre-conditioning). Then, samples were stretched at a speed of 1 % of loaded initial length (L_0) per second (typically around 0.24 mm/s). Maximal force before rupture (F_{max}) and strain at failure (S_{max}) were recorded (figure 2B). Ultimate Tensile Stress (UTS) was F_{max} divided by the cross-section area (width of the thinnest part of the dog bone (2.5 mm) multiplied by the thickness as determined by laser micrometer measurement). Young's modulus (E) was determined as the slope of the straight portion of the stress/strain curve between 4 and 5 MPa (figure 2C).

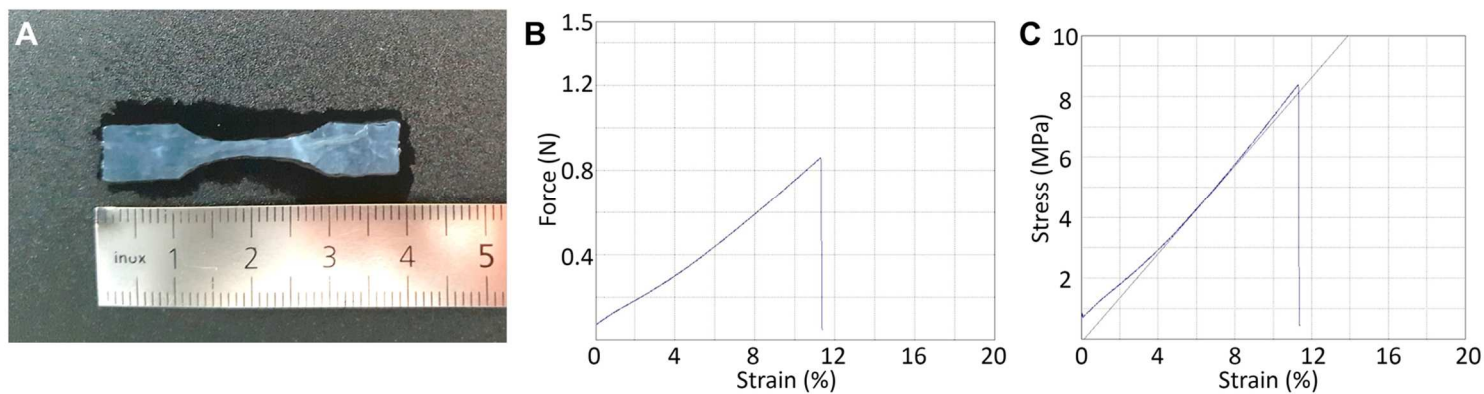


Figure 2: HAM uniaxial tensile test.

(A) Uniaxial tensile tests were performed on dog-bone shaped HAM sample. (B) and (C) Typical representation of force/strain (B) and stress/strain (C) curves obtained after testing. Young's modulus (E) was determined as the slope of the straight portion of the stress/strain curve between 4 and 5 MPa.

4.6 Statistical analysis

Data are presented as mean \pm standard deviation, with n indicating the number of HAM sample tested. If data followed Gaussian distribution (D'Agostino and Pearson omnibus normality test), differences were assessed by two-tailed t-test. Otherwise, they were assessed by the Mann and Whitney test. In both cases, differences were considered statistically significant when $p < 0.05$.

5. Results

Masson's trichrome staining of cross sections of paraffin-embedded HAM samples showed 3 layers: 1) a monolayer of epithelial cells, 2) a thin compact, acellular, collagen-rich, conjunctive layer, and 3) a thick loose layer sparsely populated with fibroblasts (figure 3A). This loose conjunctive layer could be partly removed by gentle manual scraping (figure 3B). Since it was not possible to control the amount of loose tissue left on the HAM, the thickness of the tissue was unpredictable making thickness-dependent values, such as the Ultimate Tensile Stress (UTS) and Young's modulus (E), highly unreliable. We hypothesized that the loose tissue was mostly water and did not contribute much structural collagenous material, and hence, that thickness-dependent values were meaningless in this analysis. To test this idea, HAM samples scraped to various thicknesses (ranging from 22 to 143 μm) were dehydrated while their thickness was measured continuously (figure 3C). Despite their very different starting hydrated thicknesses, dried sample thicknesses varied only from 4 to 5 μm ($4.5 \pm 0.6 \mu\text{m}$), suggesting that wet tissue thickness was not proportional to the amount of structural material present. We then compared the mechanical properties of scraped (thin) and unscraped HAM (thick), sampled next to each other on the same HAM, using a uniaxial tensile test. No statistically significant difference in both maximal force (F_{max}) and strain at break (S_{max}) was observed due to scrapping (figures 3D and 3E). However, when evaluating classic material properties, which are calculated based on tissue thickness (UTS and E), we observed clear significantly different values (figures 3F and 3G). These results showed that, because of the heterogeneity of the tissue's layered structure, UTS and E are not representative of HAM mechanical properties, which was likely provided by the compact conjunctive layer. Thus, maximal force (F_{max}) and strain at break (S_{max}) were selected to investigate HAM mechanical properties in the rest of our study.

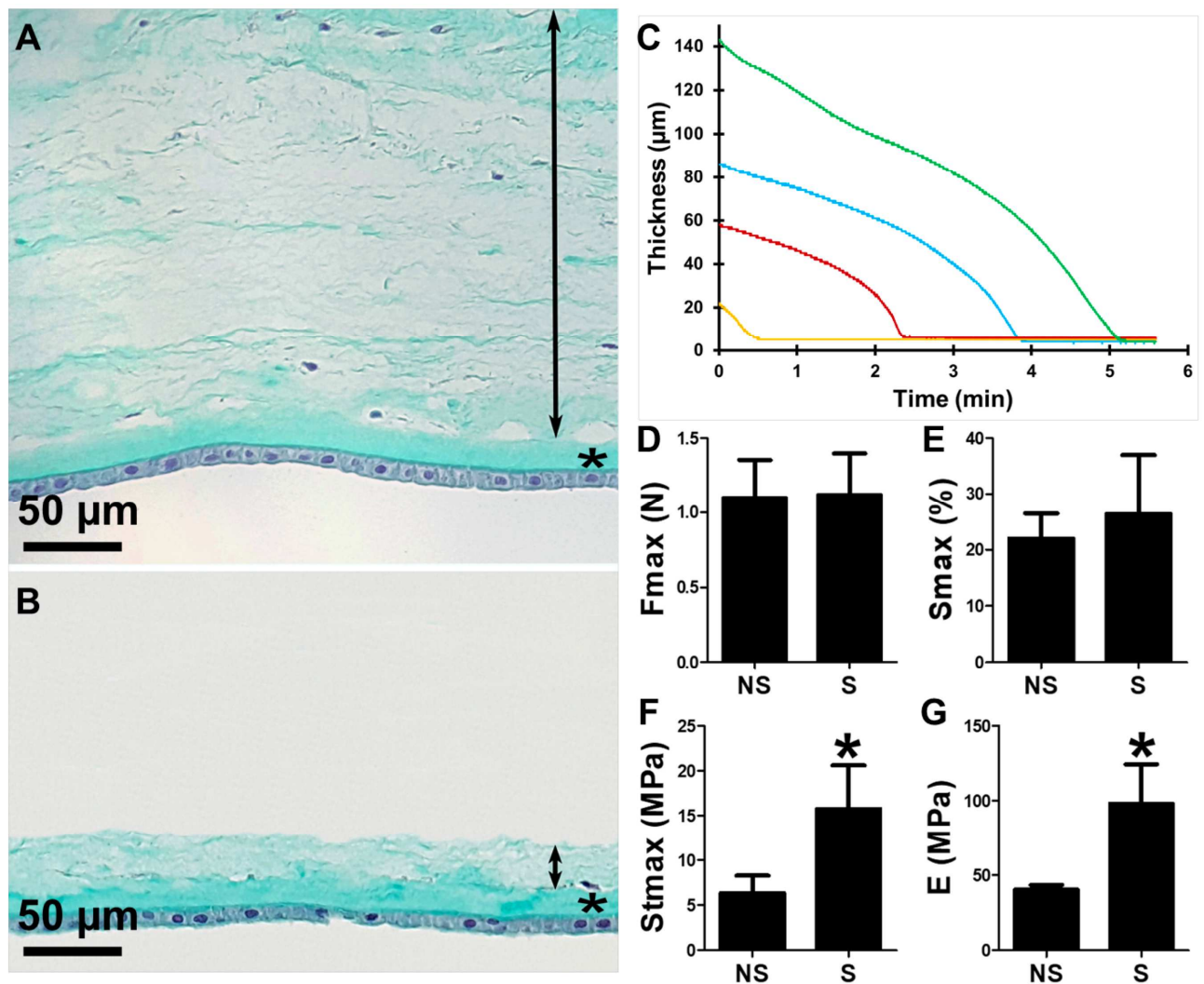


Figure 3: Structure and mechanical properties of scraped and non-scraped HAM.

(A-B) Masson's trichrome staining of cross sections of paraffin-embedded peripheral HAM samples showed a thick loose conjunctive layer (arrow), a small compact conjunctive layer (*) and an epithelial monolayer. (B) This loose layer could be partially removed by gentle manual scraping. (C) Thickness as a function of time during the dehydration of HAM samples scraped to various starting thicknesses (ranging from 22 to 143 μm). Each color is a HAM sample. Dried samples thickness varied only from 4 to 5 μm ($4.5 \pm 0.6 \mu\text{m}$). (D-E) Direct tensile mechanical properties (force (F_{max}) and strain at break (S_{max})) of scraped (S) and non-scraped samples (NS) were not statistically different. (F-G) Scraping significantly increased thickness-dependent properties like Ultimate Tensile Stress (UTS) and Young's modulus (E). Data are means \pm SD, $n = 4$ HAM samples, * indicates $p < 0.05$.

Eight HAMs were mechanically cartographed using our standardized cutting protocol and dense sampling pattern (figure 3A-H). Sociodemographic information on the patient's tissue are presented in table 1.

	Age (year)	Gravidity	Parity
HAM 1	28	5	2
HAM 2	27	2	0
HAM 3	29	3	2
HAM 4	34	2	1
HAM 5	34	1	0
HAM 6	37	2	1
HAM 7	34	4	2
HAM 8	37	9	6

Table 1: Sociodemographic informations on the patient's tissue.

On average, 103 ± 10 samples were analyzed per HAM for a total of 813 samples. However, this does not include an average of 17 ± 3 % of the samples from the preset pattern that could not be recovered due to umbilical cord insertion, surgical incision, annex placental segments, or due to damage during sampling.

Overall, the average F_{max} was 0.8 ± 0.4 N and the average S_{max} was 17 ± 3 % ($n = 813$). This overall variability, which combines inter- and intra- tissue variability, is associated with a coefficient of variation (CV%) of 46% and 20%, respectively. When data were grouped for each tissue and compared ($n = 8$), the average F_{max} was 0.83 ± 0.07 N and S_{max} was 17 ± 1 %, indicating an inter-HAM variability (of the average of all samples) of only 8.7% and 5.9%.

When we looked at the average intra-tissue variability *i.e.*, the average of the CV%s from each HAM, we obtained a value of $47\% \pm 8\%$ for Fmax and $19\% \pm 4\%$ for Smax indicating that intra-tissue variability was fairly similar in all HAMs because the variability of the variability *i.e.*, the CV% of the CV%s, was only 17% and 21%, respectively (Table 1). However, this highlighted that intra-tissue variability seemed to account for much of the overall variability, which led us to investigate if placental and peripheral areas were distinct from a mechanical point of view.

	Fmax	Smax
OVERALL VARIABILITY		
All (n = 813 samples) – CV%	46	20
Placental (n = 222 samples) – CV%	33	15
Peripheral (n = 591 samples) – CV%	37	20
INTER-TISSUE VARIABILITY (n = 8 HAMs)		
All – CV%	8.7	5.9
Placental – CV%	16	5
Peripheral – CV%	11	6
INTRA-TISSUE VARIABILITY (n = 8 HAMs)		
All – average of the CV%s (CV% of the CV%s)	47 (17)	19 (21)
Placental – average of the CV%s (CV% of the CV%s)	31 (40)	14 (18)
Peripheral – average of the CV%s (CV% of the CV%s)	37 (19)	19 (20)

Table 2: Inter- and intra- tissue variability of HAM's mechanical properties.

Figure 4 provides a visual representation of intra-tissue variability of Fmax for each HAM analysed, where sample color indicates the strength of the tissue and ranges from dark green, for the strongest sample, to red, for the weakest. In each tissue, green samples appeared concentrated in the placental area of the HAM supporting the idea that it was mechanically different than the peripheral area.

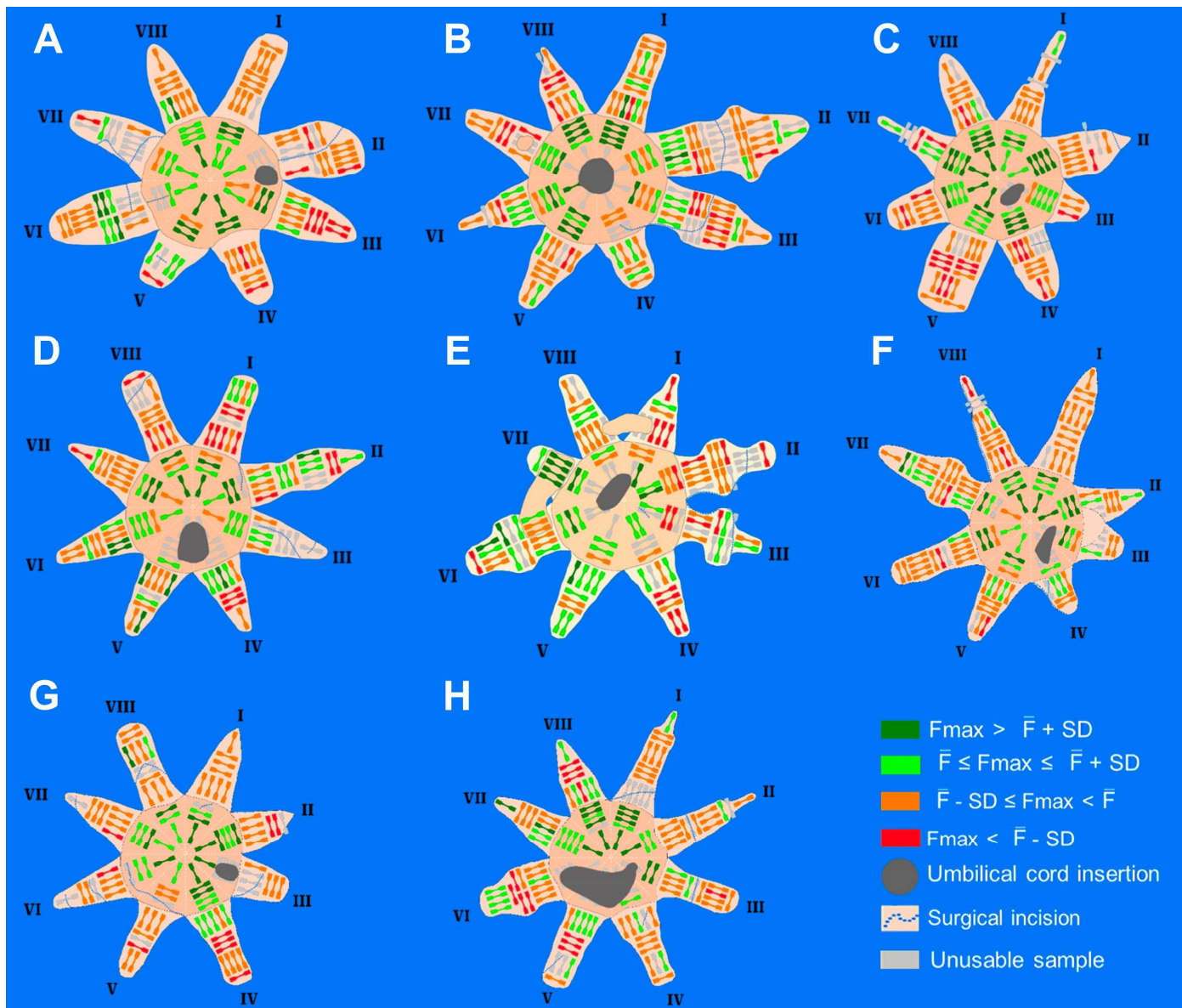


Figure 4: Schematic representation of HAM's F_{max} mechanical cartography.

(A-H) Eight HAMs were mechanically cartographed. On average, 103 ± 10 samples were analyzed per HAM with a total of 822 samples. Sample color indicates tissue strength (F_{max}) ranging from dark green ($F_{max} > \text{mean force} + SD$) to red ($F_{max} < \text{mean force} - SD$). Green and orange samples correspond to $\text{mean force} \leq F_{max} \leq \text{mean force} + SD$ and to $\text{mean force} - SD \leq F_{max} \leq \text{mean force}$, respectively. The sampling pattern described in figure 1 had to be adapted to each case because of sample loss due to umbilical cord insertion (black dot) or surgical incision (blue dotted line). Samples which could not be recovered are colored in grey.

Statistical analysis confirmed that, for all HAMs, placental HAM was significantly stronger than peripheral HAM by an average of $82\% \pm 45\%$ (range: 22% to 133%) with an average F_{max} of 1.2 ± 0.2 (CV% = 16%, range: 0.9 to 1.5 N, n = 8 HAMs) and of 0.68 ± 0.08 (CV% = 11%, range: 0.6 to 0.9 N, n = 8 HAMs), respectively (figure 5A). All placental HAMs were also significantly more stretchable than their peripheral counterparts by an average of $19\% \pm 6\%$ (range: 11% to 29%) with an average S_{max} of $19\% \pm 3\%$ (CV% = 5%, range: 18 to 21%, n = 8 HAMs) and $16\% \pm 1\%$ (CV% = 6%, range: 15 to 18%, n = 8 HAMs), respectively (figure 5B). These results were consistent with macroscopic observations (figure 1B), which showed that placental HAM was more opaque indicating that it was possibly denser. This was confirmed by histological analysis. Masson's trichrome staining of cross sections of paraffin-embedded placental HAM showed that both the loose and compact conjunctive layers were richer in collagen than placental HAM as indicated by the semi-quantitatively more intense collagen-specific green staining (figure 5C vs. figure 3B).

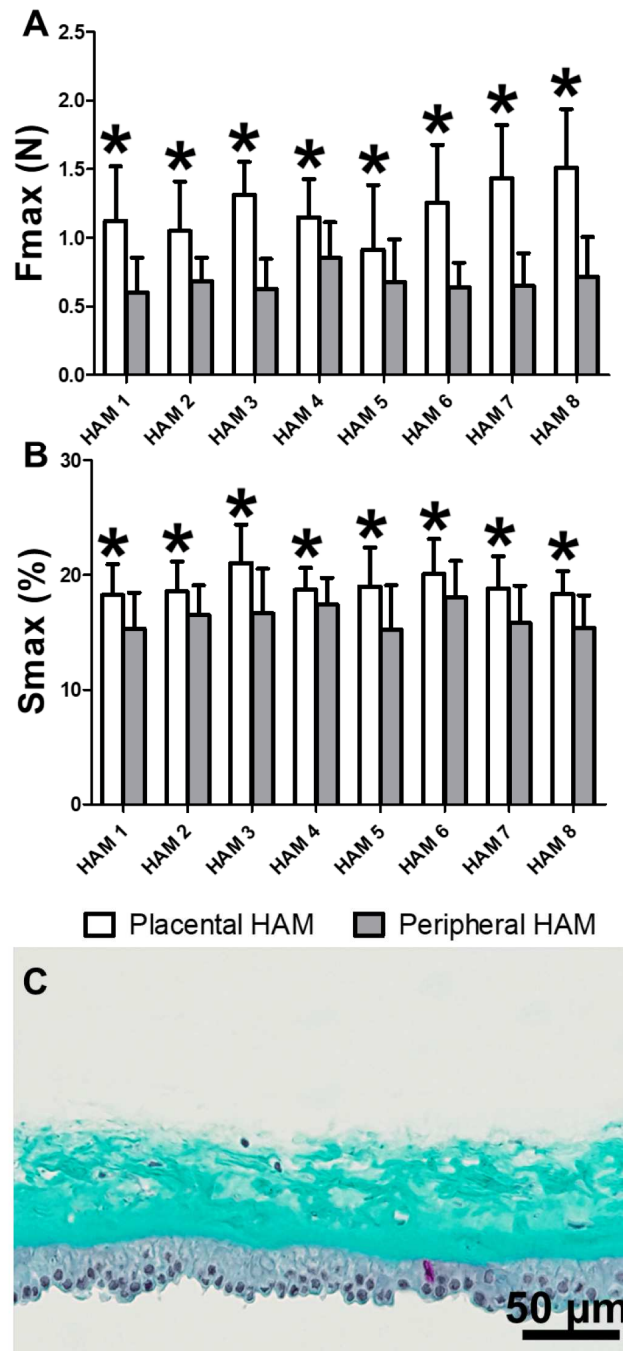


Figure 5: Differences between placental and peripheral HAM in terms Fmax, Smax, and structure. (A-B) Placental HAM (white column) was 82 ± 45 % stronger and 19 ± 6 % more stretchable than peripheral HAM (grey column). Data are means \pm SD, n placental = 222 samples (min = 21, max = 39) and n peripheral = 591 samples (min = 61, max = 94), * indicates $p < 0.05$. (C) Masson's trichrome staining of a cross section of paraffin-embedded scraped placental HAM showed a loose and a compact conjunctive layer which were both very richer in collagen (more intense green staining) than peripheral HAM (figure 3B).

The average intra-tissue variability *i.e.*, the average of the CV%s ($n = 8$), calculated for each area was $31\% \pm 13\%$ (Fmax) and $14\% \pm 3\%$ (Smax) for placental, and $37\% \pm 7\%$ (Fmax) and $19\% \pm 7\%$ (Smax) for peripheral, which was generally lower than the overall intra-tissue variability (47% and 19%). The variability of the intra-tissue variability *i.e.*, CV% of CV%s, was 40% (Fmax) and 18% (Smax) for placental, and 19% (Fmax) and 20% (Smax) for peripheral, which were similar to the values for whole HAM (17% and 21%), except for the 40%. The inter-tissue variability for each area was 16% (Fmax) and 5.1% (Smax) for placental, and 11% (Fmax) and 6.5% (Smax) for peripheral, which, surprisingly, were higher than Fmax or equivalent to Smax values of the inter-tissue variability calculated without regard for HAM area sampling (8.7% and 5.9%, respectively) (Table 1). Taken together, this data suggests that, even when accounting for sampling area, intra-tissue variability appears to be the more important contributor to overall variability.

Next, the role of sample orientation on HAM mechanical properties was studied. For placental HAM, there was no difference between radial and circumferential samples for both Fmax and Smax (figures 6A and 6B). However, in peripheral HAM, radial samples were statistically stronger than the circumferential in 5 out of 8 HAMs by an average of $37\% \pm 16\%$ (figure 6C). In terms of stretchability, sample orientation had no effect on peripheral HAM except for one case where the circumferential samples were more stretchable (figure 6D). Taken together, these results demonstrate that placental HAM is an isotropic tissue that is stronger and more stretchable than peripheral HAM whose isotropy is not always guaranteed.

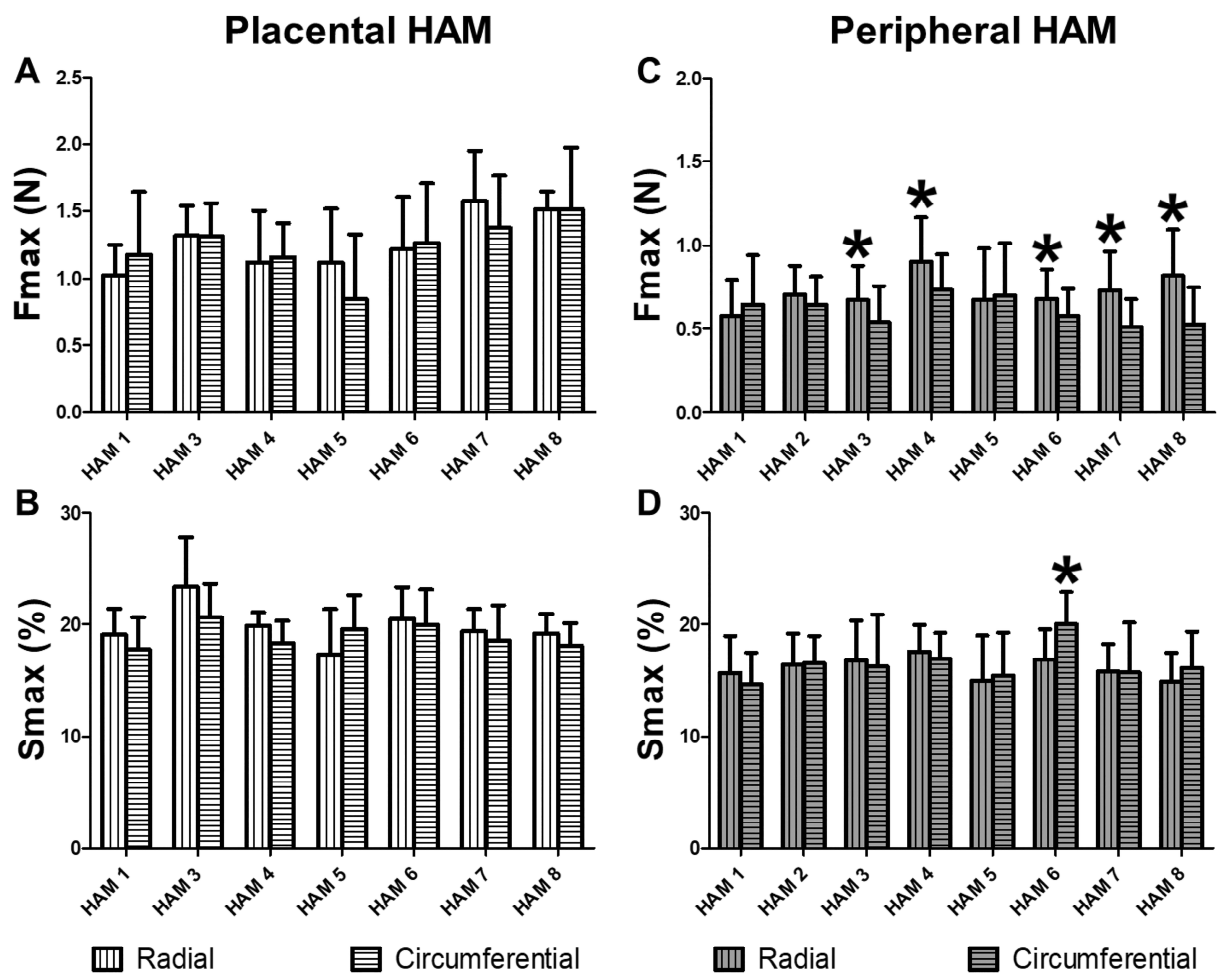


Figure 6: Effect of sample's orientation on both Fmax and Smax.

(A-B) In placental HAM, no orientation effect was observed between radial (vertical hatches on white fill) and circumferential samples (horizontal hatches on white fill) in terms of Fmax and Smax. (C) However, in peripheral HAM, the radial samples (vertical hatches on grey fill) were stronger than the circumferential samples (horizontal hatches on grey fill) in 5 HAMs out of 8. (D) Moreover, sample orientation had no effect on stretchability except for HAM n°6 where the circumferential samples were more stretchable. Data are means \pm SD, n radial = 423 samples (min = 42, max = 59) and n circumferential = 390 samples (min = 41, max = 66), * indicates $p < 0.05$.

6. Discussion

Thanks to its low immunogenicity, biological properties, and high availability, the HAM is widely used in the clinic and in tissue engineering research³⁰. However, while its biological characteristics are well described^{3 8 30}, its mechanical properties remain understudied⁹. Thus, in order to help guide tissue engineers in their use of this tissue for the development of products where mechanical properties are critical, this study was performed to generate a detailed cartography of the HAM's mechanical properties. While fresh HAM is sometimes used in the clinic, commercial surgical products are typically treated using various, undisclosed, protocols that can include steps of decellularization, lyophilization, and sterilization¹⁵. In tissue engineering, HAM treatments are usually less extensive but also vary widely^{15, 29}. Considering that there are no standard HAM processing protocols, we chose to work on the raw material (fresh HAM). We would expect that the regional variations in mechanical properties of the raw material would translate to the treated HAM but this hypothesis should be confirmed experimentally in future studies. Besides, as the benefits of working with intact or minimally treated ECM are becoming more recognized, characterization of the intact HAM may be more relevant to some investigators^{1, 12, 35}.

Prior to performing the mechanical cartography, relevant mechanical criteria were first determined. Combined analysis of histological sections, thickness measurements after dehydration, and uniaxial tensile tests, led us to select maximal force (Fmax) and strain at break (Smax) as the appropriate values to investigate HAM mechanical properties. Other groups have also used these two (or similar) thickness-independent parameters to evaluate the mechanical characteristics of the HAM²⁹. However, some studies used Ultimate Tensile Stress (UTS) and Young's Modulus (E) instead of, or in addition to, force and strain at failure^{5 16 32}. Nevertheless, our data clearly show how UTS or E evaluated on this heterogeneous multilayered tissue are: 1) only "apparent" values and not material properties, 2) are extremely dependent on the presence of loose connective tissue, which will vary greatly from operator to operator. Indeed, the large variability of HAM thickness is clearly visible in the literature where some investigators report values of 20 μm ⁵, 44 μm ³², 80 μm ²⁹, or even 111 μm ¹⁶. While some of these differences can be related to the various measurement methods

used, Jabareen *et al.* measured the thickness of 9 HAMs and reported a range of 43 to 305 μm and a standard deviation of 78 (CV% = 70%). This clearly suggests that UTS and E are poor values to describe HAM mechanical properties.

A standardized cutting protocol and a dense sampling pattern were developed for the mechanical cartography of the HAM. To our knowledge, El Khwad *et al.* published the only mechanical cartography of the HAM⁹. Although that study involved a slightly higher patient number than our (12 vs. 8 in our study), their sampling pattern used very large samples and, as a result, had a small number of samples per HAM (13 samples vs. more than 100 in our study). In addition, the study used a perforation test, which does not give comparable tensile data or information on the isotropy of the tissue. Finally, that study did not investigate the properties of the placental HAM.

To understand the process of fetal membrane rupture, a natural and necessary event of the delivery process, scientists have shown that, in peripheral HAM, there was a distinct weak zone overlying the *cervix* with particular biochemical and histological features^{9 25 26}. Despite the high resolution of our sampling, we did not locate this weak zone. We hypothesize that, this area was not identified because it was along the tear created when the obstetric surgeon widened his surgical incisions. It would make sense that this weak region would preferentially propagate the initial cut during the stretching of the membranes at the end of a cesarean delivery. Since we did not get access to the fetal bag prior to delivery to stain the region above the *cervix* to be able to locate it at the time of sampling, this question still remains a hypothesis.

The average tensile F_{max} (0.83 ± 0.07 N, $n = 8$ HAMs) was roughly twice that of the value reported by Oxlund *et al.* (0.4 ± 0.3 N)³². Note that the samples tested by Oxlund *et al.* were 4 mm wide strips so we normalized their values to account for this difference in width. Also, the standard deviation was calculated from the standard error of the mean reported in their study with an $n = 6$. Similar values can be calculated from the data reported by Niknejad *et al.* for fresh and glycerol-frozen HAM (≈ 0.4 N and 0.2 N respectively)²⁹. An approximate F_{max} value of ≈ 0.6 N can be calculated from the data of Chuck *et al.*⁵. The higher F_{max} from our study is partially due to the fact

that some of our samples came from placental HAM (27%), unlike the cited studies which focused exclusively on peripheral HAM. The average F_{max} for peripheral HAM only was 0.68 ± 0.08 N, which is still generally higher than published data. This may be due, in part, to the fact that these studies used strips, which would normally break at lower values than the dog-bone shaped samples we used. Since strain rate can influence the breaking strength, we hypothesize that this variable might also contribute to our higher values. Only Oxlund *et al.* provided sufficient data to establish the strain rate used, which we calculated to be $2.4\% \text{ s}^{-1}$ ³². Considering that we used a $1\% \text{ s}^{-1}$ strain rate and that breaking strength increases with the testing strain rate ³¹, this difference in strain rate could only explain a higher F_{max} for Oxlund *et al.* This suggests that both strain rates represent quasi-static testing conditions.

The average S_{max} for peripheral samples was $16\% \pm 1\%$, which was roughly half that of Oxlund *et al.*, the only study we found that measured strain at break. This difference is surprising because stronger tissues can generally be stretched more before breaking and our F_{max} was roughly twice that of Oxlund *et al.* ^{5 29}. This apparent discrepancy could be due to the fact that this group did not use any pre-loading or mechanical pre-conditioning. As a result, their L_0 was measured on a very loose tissue while the L_0 we used was measured on a tissue loaded with 0.1N. This would allow for an important displacement before equivalent loading of the tissue and result in a larger displacement before failure (D_f). As a result, the S_{max} would be overestimated due to both a higher displacement at break and a shorter L_0 since $S_{max} = L_0 + D_f / L_0$. However, in retrospect, our use of 0.1 N as a pre-load might have been excessive since it represents close to 10% of the F_{max} .

The novelty of this study was to describe the important mechanical difference between peripheral and the often-forgotten placental HAM. The differences between these two areas in terms of transparency ⁶, histological structure ^{2 13}, metabolic activity ² and gene expression ¹³ have already been reported. However, to our knowledge, no study has compared their mechanical properties. Our results demonstrated that placental HAM was always stronger, by an average of $82 \pm 45 \%$, and more stretchable, by an average of $19 \pm 6 \%$, than peripheral HAM. This data was consistent with the richer collagen structure of the placental HAM revealed by histology. These data are supported by

those obtained by Jabareen *et al.* who found that inter-tissue (patient-to-patient) variability in peripheral HAM strength could be explained by collagen content differences¹⁶ For placental human amniotic membrane, Fmax and Smax varied in the same direction although it is not always the case with all tissues.

Another novel aspect of our study was that we investigated the isotropy of this material. Because the fetal bag might be exposed to directional forces due to the fetus' movements, we looked at the influence of sample orientation on mechanical properties. We used samples that were in the axis that goes from the placenta to the opposite side of the fetal bag (radial samples), and samples that were taken perpendicularly to that direction (circumferential). We demonstrated that, in all HAMs, placental sampling was not sensitive to orientation in term of Fmax and Smax. However, in peripheral HAM, radial samples were significantly stronger than circumferential samples in 5 out of 8 HAMs (by 37 ± 16 %). These results could be explained by the fact that the HAM covering the placenta is mechanically connected to the very thick placenta, which could shield it from deformations caused by the fetus pushing on the fetal membranes. The peripheral HAM would not benefit from such a mechanical support and would likely be more exposed to deformations and stress. In addition, because the peripheral HAM is more mobile and the placental more tethered, we would expect tension to develop preferentially along lines going from the more mobile towards the less mobile tissue. This could result in the alignment of collagen fibers along these stress lines, *i.e.* in the radial orientation. This would explain why radial samples were generally stronger than circumferential samples only in the peripheral HAM. In only 1 out of 8 cases, the circumferential peripheral samples were more stretchable. We attribute this observation to a non-homogenous and exceptional distribution that caused a statistical anomaly. This lack of increased stretchability at failure might seem surprising since stronger tissues are typically more stretchable. However, this generalization is made when stronger tissues are thicker or denser. If we suppose that the increased strength of the tissue is only due to a collagen fiber reorganization, one would not expect the tissue to be more stretchable (on the contrary).

Inter-tissue (patient-to-patient) variability was surprising low even when we compared HAM values that combined peripheral and placental tissues (CV% = 8.7% for Fmax and 5.9% for Smax). Even more surprising was that inter-tissue variability was somewhat higher (for Fmax), or very similar (for Smax), when we analyzed data separately for placental (CV% = 16% and 5.1%, respectively) and peripheral areas (CV% = 11% and 6.5%, respectively), suggesting that intra-tissue variability accounts for most of the overall variability. Indeed, intra-tissue variability for each area was $33\% \pm 13\%$ (Fmax) and $14\% \pm 3\%$ (Smax) for placental, and $37\% \pm 7\%$ (Fmax) and $19\% \pm 7\%$ (Smax), which account for most of the overall variability of 46% (Fmax) and 20% (Smax). This variability analysis confirms that sourcing material from multiple HAMs only marginally increases tissue variability and can be considered a sound strategy.

7. Conclusions

This study, based on the analysis of more than 800 samples, is the most detailed cartography of the HAM's mechanical properties. We have quantified the inter- and intra-tissue variability in terms of strength and stretchability in order to allow tissue engineers to make informed design decisions when using HAM as a scaffold. We show for the first time that strength, stretchability, and isotropy are superior in the placental compared to peripheral HAM. Thus, although the placental HAM is often neglected because of its smaller size and its less homogenous appearance, it offers specific mechanical properties. Placental HAM can be, therefore, a raw material of choice that could be favored especially in the development of tissue engineering products where mechanical properties play a key role.

8. Acknowledgements

The authors would like to acknowledge Patrick Guitton for his technical help.

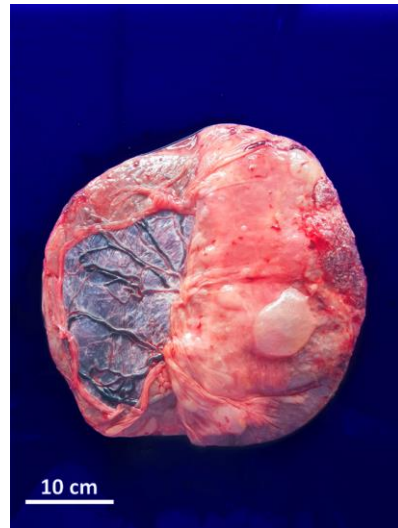
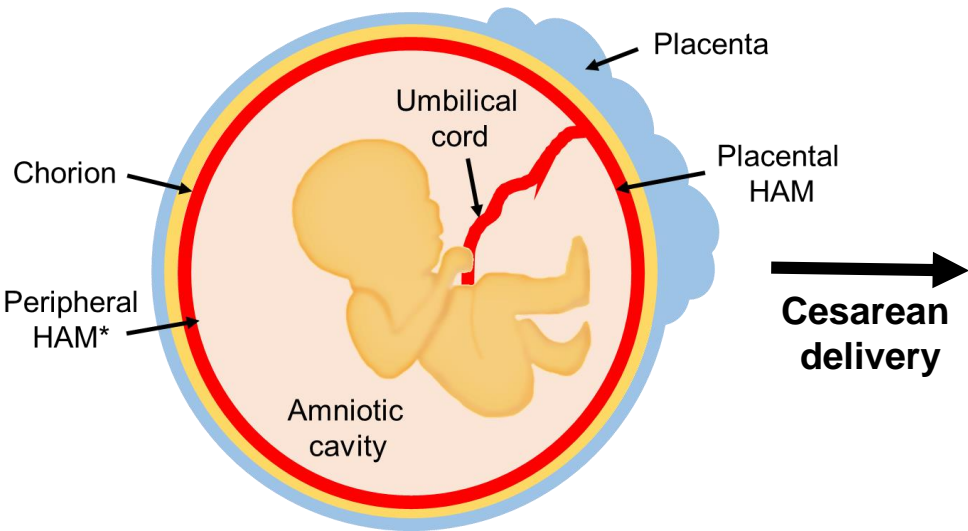
This research did not receive any specific grant from funding agencies in the public, commercial, or not-for-profit sectors.

Declarations of interest: none.

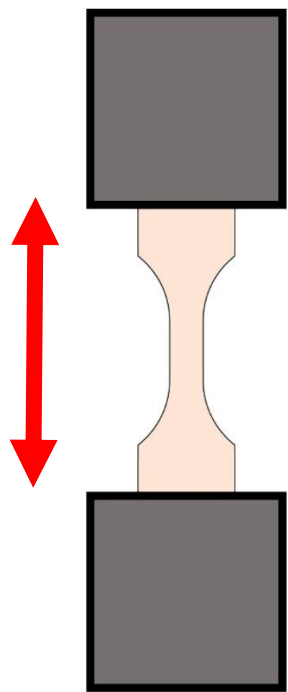
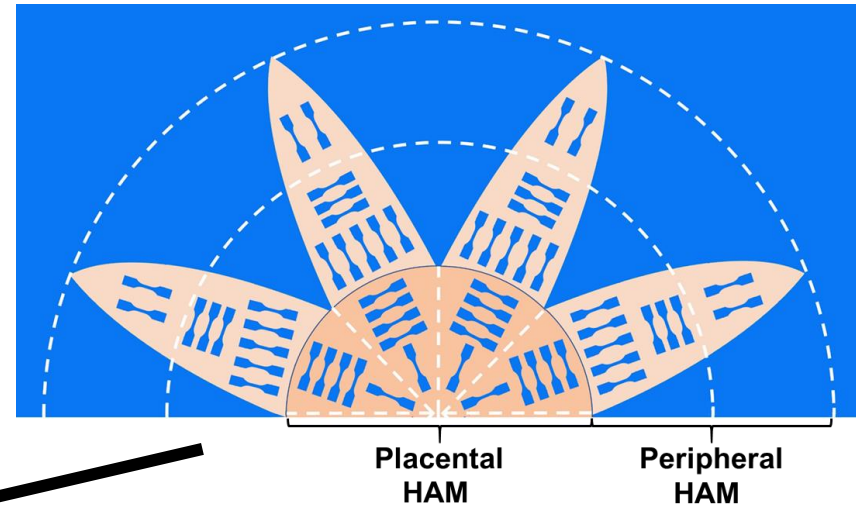
9. References

1. Amensag S., L. Goldberg, K. A. O'Malley, D. S. Rush, S. A. Berceli and P. S. McFetridge. Pilot assessment of a human extracellular matrix-based vascular graft in a rabbit model. *J Vasc Surg* 65: 839-847 e831, 2017.
2. Banerjee A., A. Weidinger, M. Hofer, R. Steinborn, A. Lindenmair, S. Hennerbichler-Lugscheider, J. Eibl, H. Redl, A. V. Kozlov and S. Wolbank. Different metabolic activity in placental and reflected regions of the human amniotic membrane. *Placenta* 36: 1329-1332, 2015.
3. Bourne G. The foetal membranes. A review of the anatomy of normal amnion and chorion and some aspects of their function. *Postgrad Med J* 38: 193-201, 1962.
4. Buerzle W. and E. Mazza. On the deformation behavior of human amnion. *J Biomech* 46: 1777-1783, 2013.
5. Chuck R. S., J. M. Graff, M. R. Bryant and P. M. Sweet. Biomechanical characterization of human amniotic membrane preparations for ocular surface reconstruction. *Ophthalmic Res* 36: 341-348, 2004.
6. Deihim T., G. Yazdanpanah and H. Niknejad. Different Light Transmittance of Placental and Reflected Regions of Human Amniotic Membrane That Could Be Crucial for Corneal Tissue Engineering. *Cornea* 35: 997-1003, 2016.
7. Diaz-Prado S., M. E. Rendal-Vazquez, E. Muinos-Lopez, T. Hermida-Gomez, M. Rodriguez-Cabarcos, I. Fuentes-Boquete, F. J. de Toro and F. J. Blanco. Potential use of the human amniotic membrane as a scaffold in human articular cartilage repair. *Cell Tissue Bank* 11: 183-195, 2010.
8. Dobрева M. P., P. N. Pereira, J. Deprest and A. Zwijsen. On the origin of amniotic stem cells: of mice and men. *Int J Dev Biol* 54: 761-777, 2010.
9. El Khwad M., B. Stetzer, R. M. Moore, D. Kumar, B. Mercer, S. Arikat, R. W. Redline, J. M. Mansour and J. J. Moore. Term human fetal membranes have a weak zone overlying the lower uterine pole and cervix before onset of labor. *Biol Reprod* 72: 720-726, 2005.
10. Fenelon M., S. Catros and J. C. Fricain. What is the benefit of using amniotic membrane in oral surgery? A comprehensive review of clinical studies. *Clin Oral Investig* 22: 1881-1891, 2018.
11. Fenelon M., O. Chassande, J. Kalisky, F. Gindraux, S. Brun, R. Bareille, Z. Ivanovic, J. C. Fricain and C. Boiziau. Human amniotic membrane for guided bone regeneration of calvarial defects in mice. *J Mater Sci Mater Med* 29: 78, 2018.
12. Gui L., A. Muto, S. A. Chan, C. K. Breuer and L. E. Niklason. Development of decellularized human umbilical arteries as small-diameter vascular grafts. *Tissue Eng Part A* 15: 2665-2676, 2009.
13. Han Y. M., R. Romero, J. S. Kim, A. L. Tarca, S. K. Kim, S. Draghici, J. P. Kusanovic, F. Gotsch, P. Mittal, S. S. Hassan and C. J. Kim. Region-specific gene expression profiling: novel evidence for biological heterogeneity of the human amnion. *Biol Reprod* 79: 954-961, 2008.
14. Hao Y., D. H. Ma, D. G. Hwang, W. S. Kim and F. Zhang. Identification of antiangiogenic and antiinflammatory proteins in human amniotic membrane. *Cornea* 19: 348-352, 2000.
15. Ilic D., L. Vicovac, M. Nikolic and E. Lazic Ilic. Human amniotic membrane grafts in therapy of chronic non-healing wounds. *Br Med Bull* 117: 59-67, 2016.
16. Jabareen M., A. S. Mallik, G. Bilic, A. H. Zisch and E. Mazza. Relation between mechanical properties and microstructure of human fetal membranes: an attempt towards a quantitative analysis. *Eur J Obstet Gynecol Reprod Biol* 144 Suppl 1: S134-141, 2009.
17. Joyce E. M., J. J. Moore and M. S. Sacks. Biomechanics of the fetal membrane prior to mechanical failure: review and implications. *Eur J Obstet Gynecol Reprod Biol* 144 Suppl 1: S121-127, 2009.
18. King A. E., A. Paltoo, R. W. Kelly, J. M. Sallenave, A. D. Bocking and J. R. Challis. Expression of natural antimicrobials by human placenta and fetal membranes. *Placenta* 28: 161-169, 2007.
19. Kjaergaard N., M. Hein, L. Hyttel, R. B. Helmig, H. C. Schonheyder, N. Uldbjerg and H. Madsen. Antibacterial properties of human amnion and chorion in vitro. *Eur J Obstet Gynecol Reprod Biol* 94: 224-229, 2001.
20. Kubo M., Y. Sonoda, R. Muramatsu and M. Usui. Immunogenicity of human amniotic membrane in experimental xenotransplantation. *Invest Ophthalmol Vis Sci* 42: 1539-1546, 2001.

21. Li W., G. Ma, B. Brazile, N. Li, W. Dai, J. R. Butler, A. A. Claude, J. A. Wertheim, J. Liao and B. Wang. Investigating the Potential of Amnion-Based Scaffolds as a Barrier Membrane for Guided Bone Regeneration. *Langmuir* 31: 8642-8653, 2015.
22. Magatti M., E. Vertua, S. De Munari, M. Caro, M. Caruso, A. Silini, M. Delgado and O. Parolini. Human amnion favours tissue repair by inducing the M1-to-M2 switch and enhancing M2 macrophage features. *J Tissue Eng Regen Med* 11: 2895-2911, 2017.
23. Malhotra C. and A. K. Jain. Human amniotic membrane transplantation: Different modalities of its use in ophthalmology. *World J Transplant* 4: 111-121, 2014.
24. Mauri A., A. E. Ehret, M. Perrini, C. Maake, N. Ochsenbein-Kolble, M. Ehrbar, M. L. Oyen and E. Mazza. Deformation mechanisms of human amnion: Quantitative studies based on second harmonic generation microscopy. *J Biomech* 48: 1606-1613, 2015.
25. McLaren J., T. M. Malak and S. C. Bell. Structural characteristics of term human fetal membranes prior to labour: identification of an area of altered morphology overlying the cervix. *Hum Reprod* 14: 237-241, 1999.
26. McParland P. C., D. J. Taylor and S. C. Bell. Mapping of zones of altered morphology and chorionic connective tissue cellular phenotype in human fetal membranes (amniochorion and decidua) overlying the lower uterine pole and cervix before labor at term. *Am J Obstet Gynecol* 189: 1481-1488, 2003.
27. Mligiliche N., K. Endo, K. Okamoto, E. Fujimoto and C. Ide. Extracellular matrix of human amnion manufactured into tubes as conduits for peripheral nerve regeneration. *J Biomed Mater Res* 63: 591-600, 2002.
28. Mohan R., A. Bajaj and M. Gundappa. Human Amnion Membrane: Potential Applications in Oral and Periodontal Field. *J Int Soc Prev Community Dent* 7: 15-21, 2017.
29. Niknejad H., T. Deihim, M. Solati-Hashjin and H. Peirovi. The effects of preservation procedures on amniotic membrane's ability to serve as a substrate for cultivation of endothelial cells. *Cryobiology* 63: 145-151, 2011.
30. Niknejad H., H. Peirovi, M. Jorjani, A. Ahmadiani, J. Ghanavi and A. M. Seifalian. Properties of the amniotic membrane for potential use in tissue engineering. *Eur Cell Mater* 15: 88-99, 2008.
31. Ottenio M., D. Tran, A. Ni Annaidh, M. D. Gilchrist and K. Bruyere. Strain rate and anisotropy effects on the tensile failure characteristics of human skin. *J Mech Behav Biomed Mater* 41: 241-250, 2015.
32. Oxlund H., R. Helmig, J. T. Halaburt and N. Uldbjerg. Biomechanical analysis of human chorioamniotic membranes. *Eur J Obstet Gynecol Reprod Biol* 34: 247-255, 1990.
33. Oyen M. L., R. F. Cook and S. E. Calvin. Mechanical failure of human fetal membrane tissues. *J Mater Sci Mater Med* 15: 651-658, 2004.
34. Peirovi H., N. Rezvani, M. Hajinasrollah, S. S. Mohammadi and H. Niknejad. Implantation of amniotic membrane as a vascular substitute in the external jugular vein of juvenile sheep. *J Vasc Surg* 56: 1098-1104, 2012.
35. Wystrychowski W., T. N. McAllister, K. Zagalski, N. Dusserre, L. Cierpka and N. L'Heureux. First human use of an allogeneic tissue-engineered vascular graft for hemodialysis access. *J Vasc Surg* 60: 1353-1357, 2014.



HAM cutting and sampling



Uniaxial tensile test

Results

<p>Placental HAM:</p> <ul style="list-style-type: none"> • Stronger • More stretchable • Isotropic 	<p>Peripheral HAM:</p> <ul style="list-style-type: none"> • Weaker • Less stretchable • Anisotropic
--	---

*HAM = Human Amniotic Membrane